

# Uncertainty Quantification and Optimal Design of EV-WPT System Efficiency based on Adaptive Gaussian Process Regression

Xinlei Shang<sup>1</sup>, Linlin Xu<sup>1</sup>, Quanyi Yu<sup>1</sup>, Bo Li<sup>1</sup>, Gang Lv<sup>2</sup>, Yaodan Chi<sup>3</sup>, and Tianhao Wang<sup>1\*</sup>

<sup>1</sup>College of Instrument and Electrical Engineering

Jilin University, Changchun, 130026, China

shangxinlei@jlu.edu.cn, xull21@mails.jlu.edu.cn, qyyu20@mails.jlu.edu.cn,

libo21@mails.jlu.edu.cn, \*wangtianhao@jlu.edu.cn

<sup>2</sup>EMC Department National Automotive Quality Supervision and Inspection Center

Changchun, 130011, China

lvgang@catc.com.cn

<sup>3</sup>Jilin Provincial Key Laboratory of Architectural Electricity and Comprehensive Energy Saving

Jilin Jianzhu University Changchun, 130118, China

chiyaodan@jlju.edu.cn

**Abstract** – Wireless power transfer (WPT) is a safe, convenient, and intelligent charging solution for electric vehicles. To address the problem of the susceptibility of transmission efficiency to large uncertainties owing to differences in coil and circuit element processing and actual driving levels, this study proposes the use of adaptive Gaussian process regression (aGPR) for the uncertainty quantification of efficiency. A WPT system efficiency aGPR surrogate model is constructed with a set of selected small-sample data, and the confidence interval and probability density function of the transmission efficiency are predicted. Finally, the reptile search algorithm is used to optimize the structure of the WPT system to improve efficiency.

**Index Terms** – Adaptive Gaussian process regression (aGPR), electric vehicle (EV), optimal design, uncertainty quantification (UQ), wireless power transfer (WPT).

## I. INTRODUCTION

With the rapid development of electric vehicle (EV) technology, its charging methods have also improved [1]. In response to the drawbacks of cable charging methods, wireless power transfer (WPT) technology was designed to remove the mechanical interface, improve safety, and enable dynamic charging. The technology is advanced, maturing gradually [2, 3], and a promising mainstream EV charging technology in the future [4]. Many scholars examined the issues related to EV-WPT systems and developed international standards [5]. However, owing to the complex design and control of the transfer system

and differences in actual driving levels, each factor in the coil structure, transfer distance, misalignment, and compensation topology design can directly or indirectly impact the efficiency of the system [6–8]. As the uncertainty of the aforementioned relevant factors as input parameters will have a significant impact on WPT system efficiency, conducting uncertainty quantification (UQ) evaluation and optimization studies on the efficiency of EV-WPT systems is important.

Parametric UQ methods include statistical and non-statistical methods, among which the statistical methods are dominated by the Monte Carlo (MC) method and its improvements, which are typically used to verify the accuracy of other UQ methods [9]. Owing to the complexity and high computational cost of an experimental system, nonstatistical methods based on the generalized polynomial chaos expansion (gPCE) method, machine learning, deep learning, and the Kriging surrogate model are widely used in UQ studies. Rossi et al. [10] combined gPCE theory with an effective model of interactions among devices in the radiative near field to build a UQ framework for the efficiency of WPT systems and demonstrated that the method is more flexible and efficient than the stochastic configuration method, based on a single gPCE and direct MC analysis; however, the mapping solving process of the PCE surrogate model suffers from the problem of the “curse of dimensionality” [11]. With the development of artificial intelligence, machine learning has gradually been employed in the field of WPT electromagnetic compatibility. Trincherio et al. [12] examined leastsquares support vector machine (LS-SVM) regression and its optimized form for WPT

efficiency UQ and demonstrated that LS-SVM regression, based on kernel technology, can effectively solve the high-dimensional spatial nonlinear UQ problem, but the hyperparameter selection lacks a priori knowledge and cannot be realized based on a rigorous mathematical basis. Larbi et al. [13] employed LS-SVM regression, combined with Gaussian process regression (GPR), for WPT system UQ. Based on the quantification results, the authors used partial least squares regression for the sensitivity analysis of the parameters and system efficiency optimization but obtained poor prediction results for the regions with a low probability of occurrence. Other scholars applied the Kriging surrogate model [14] and deep learning [15] to the UQ and optimization of simplified WPT systems, but UQ capability for the complex structure of WPT simulation models remains to be verified. The GPR method, based on Gaussian stochastic processes, kernel techniques, and Bayesian inference theory, can overcome the “curse of dimensionality” and follows a strict mathematical derivation of the hyperparameters while giving a more comprehensive uncertainty analysis than LS-SVM regression and adaptive sparse PCE [16]; however, the number of training samples can be further reduced to lessen the computational cost.

In terms of WPT efficiency optimization, Chen et al. [17] proposed a series-parallel hybrid resonant structure and optimized capacitor parameters to improve WPT efficiency while achieving a long transfer distance. Yang et al. [18] optimized the voltage gain and transmission efficiency by designing compensation parameters for series/series-parallel inductive power transfer systems. Meanwhile, Zhou et al. [19] employed a constrained adaptive particle swarm algorithm with a multi-objective function, using DC – DC input voltage as the decision variable to perform the multi-objective optimization of the output power and efficiency of a WPT system. The above studies showed that the optimization of the efficiency of WPT systems is influenced by a variety of parameters. Therefore, the optimization of EV-WPT transmission efficiency based on UQ can, on the one hand, fully consider the practical application of WPT systems and, on the other hand, provide a reference for improving the robustness of such systems.

To address the shortcomings of the above studies, an information entropy adaptive sampling strategy is used in this study to build an adaptive GPR (aGPR) surrogate model to quantify the transmission efficiency uncertainty and compare it with the MC method and GPR UQ results. Based on the UQ, the efficient reptile search algorithm (RSA) is combined to optimize the component parameters in the compensation network to improve transmission efficiency and system robustness.

The main contents of this paper are as follows: Section II introduces the EV-WPT system numerical

simulation model, and Section III builds an aGPR-based transmission efficiency UQ framework for an EV-WPT system. Section IV presents the application of the RSA in the transmission efficiency prediction and overall system optimization, and Section V describes the specific experimental procedure for verifying the UQ capability of the aGPR model and effectiveness of the optimization scheme. Finally, Section VI summarizes the whole work.

## II. NUMERICAL SIMULATION MODEL OF EV-WPT SYSTEM

Based on the principle of magnetic coupling resonance, this study uses space alternating magnetic fields to transfer power and establishes a simulation model of a magnetically coupled resonant EV-WPT system by COMSOL software. The working frequency of the system is 85kHz and the output power is 3 kW.

Figure 1 (a) presents an overall model of EVs, referring to most family car models on the market, with a design body size of 4500 mm  $\times$  2000 mm  $\times$  1500 mm and material of mainly aluminum, ignoring other non-electromagnetic materials. Figure 1 (b) shows a square magnetic coupling mechanism, the inner side of which is the power transfer coil group consisting of transmitting and receiving coils, with an outer contour size of 600 mm  $\times$  600 mm and an inner contour size of 300 mm  $\times$  300 mm. The vertical distance  $d$  of the transceiver coil is within the range of 100-150 mm, the number of turns of the coil on each side is 11, the conductor material is copper, and the radius of the cross-section  $r_0$  is 0.8 mm. The outer side of the coil group is covered with ferrite of the same size as the outer contour of the transfer coil, with a thickness of 10 mm, which can improve the coupling coefficient and reduce magnetic field leakage, thereby improving transmission efficiency. The scale factor  $l$  is

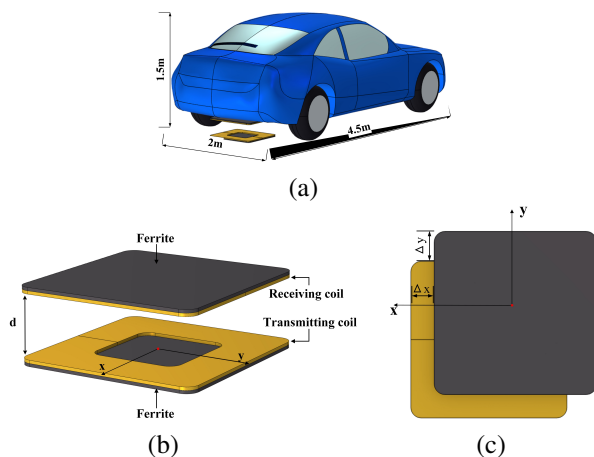


Fig. 1. EV with WPT and magnetically coupled mechanism.

defined as the scaling of the dimensions of the square transceiver coils to their square centers (e.g., the dot in Fig. 1 (b)), and  $\Delta x$  and  $\Delta y$  are the misalignment of the coupling mechanism in the horizontal x - and y-axis directions, respectively, as shown in Fig. 1 (c).

As WPT coils typically have a small coupling coefficient, S-S and parallel-series topologies are highly suitable for efficient WPT systems [20]. To further enhance the transmission power, an S-S compensation circuit is used in this study, as shown in Fig. 2, where  $I_S$  is the AC current source,  $R_T$  is the equivalent resistance of the transmitting loop,  $R_R$  is the equivalent resistance of the receiving loop,  $R_L$  is the load resistance,  $C_T$  and  $C_R$  are compensation capacitors at the transmitting and receiving end, respectively,  $L_T$  and  $L_R$  are the equivalent inductance of the transmitting and receiving coils, respectively, and  $M$  is the mutual inductance between the two coils. When resonance is generated between the two coils, the efficiency of the power transfer in the system will be [21]:

$$\eta = \frac{R_L}{R_R + R_L} \frac{\omega^2 M^2}{\omega^2 M^2 + R_T(R_R + R_L)}, \quad (1)$$

where  $R_Z = R_R + R_L$ ,  $\omega$  is the resonant angular frequency.

In practice, differences exist in the manufacturing of coils and circuit components and in the operations of the driver, which may lead to uncertainty in the coil dimensions and circuit element parameters and misalignment of the transmitting and receiving coil packs, thereby affecting the mutual inductance and mutual coupling coefficient. Such differences may also inevitably cause uncertainty in the transmission efficiency of EV-WPT systems. Therefore, typical deterministic studies are not representative, and UQ studies on EV-WPT efficiency must be conducted statistically to analyze the extent to which efficiency is affected by multiple factors. This study focuses on the UQ of EV-WPT system efficiency under misalignment, physical dimensions, and component parameters and further optimizes it. In the next section, a UQ framework for the transmission efficiency of an EV-WPT system is developed based on aGPR machine learning.

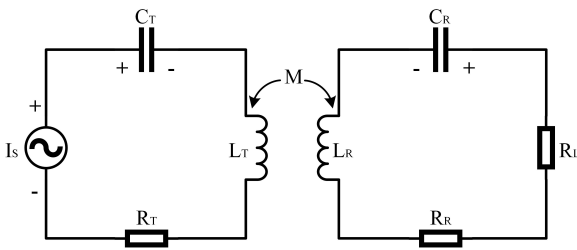


Fig. 2. Series-series (S-S) compensation circuit.

### III. UQ OF EV-WPT TRANSMISSION EFFICIENCY BASED ON AGPR

A. GPR for transmission efficiency prediction GPR is a parameter-free stochastic process regression based on a Gaussian distribution, which can give probabilistic approximate predictions on the quantity of interest and calculate the predicted variance at each sample point in the input parameter space [22]. The Gaussian process is entirely determined by the mean function (trend) and covariance function (kernel function). The hyperparameters of the covariance function can be optimized when training the GP model. This study uses GPR to establish the correspondence between the d-D column vector of input parameters  $\mathbf{x}_{p \times d}$  and transmission efficiency of the WPT system  $\boldsymbol{\eta}_{n \times 1}$ , then builds a surrogate model and quantifies the uncertainty.

Based on the function space perspective, the Gaussian process can be expressed as:

$$f(\mathbf{x}) \sim GP(m(\mathbf{x}), k_\theta(\mathbf{x}, \mathbf{x}')), \quad (2)$$

where  $\theta$  is the hyperparameter of the covariance function, and  $m(\mathbf{x})$  and  $k_\theta(\mathbf{x}, \mathbf{x}')$  are the mean and covariance functions of the stochastic process  $f(\mathbf{x})$ , respectively [23]. The GPR learning problem for transmission efficiency is:

$$\boldsymbol{\eta} = f + \boldsymbol{\varepsilon}. \quad (3)$$

The GPR training process is shown in Fig. 3, where  $f$  is considered as a potential function,  $\boldsymbol{\varepsilon}$  is the estimated noise of the GP,  $\boldsymbol{\varepsilon} \sim \mathbf{N}(0, \sigma_n^2 \mathbf{I})$ , and  $f_1, f_2, \dots, f_n$  satisfy the joint Gaussian distribution.

To simplify the calculation, let the prior trend of  $\boldsymbol{\eta}$  constructed from the  $n$  training samples ( $\mathbf{x}_{n \times d}, \boldsymbol{\eta}_{n \times 1}$ ) be  $\boldsymbol{\eta} \sim \mathbf{N}(0, K_{ff} + \sigma_n^2 \mathbf{I})$  and the potential function constructed from the  $m$  testing samples be  $f^*$ . The joint prior distribution of  $\boldsymbol{\eta}$  and  $f^*$  is:

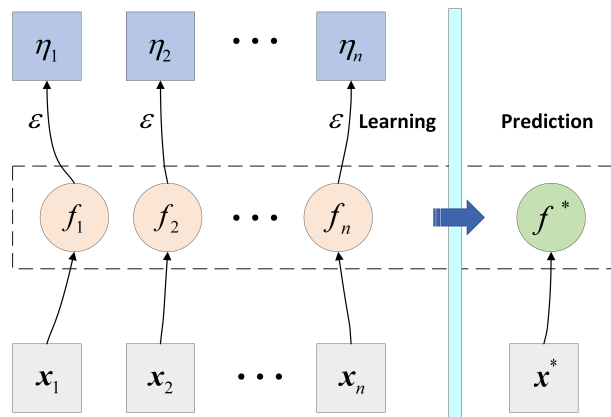


Fig. 3. GPR prediction process for transmission efficiency.

$$\begin{bmatrix} \boldsymbol{\eta} \\ \mathbf{f}^* \end{bmatrix} \sim N\left(\mathbf{0}, \begin{bmatrix} \mathbf{K}_{ff} + \sigma_n^2 \mathbf{I} & \mathbf{K}_{ff}^T \\ \mathbf{K}_{ff} & \mathbf{K}_{\psi^*} \end{bmatrix}\right) \quad (4)$$

where  $\mathbf{K}_{ff}, \mathbf{K}_{**}, \mathbf{K}_{ff^*}$  are the covariance matrices between the training samples, testing samples, and the training and testing samples, respectively. The mean  $\bar{f}^*$  and variance  $\sigma_*^2$  of the predicted distribution can be derived from Bayesian theory as:

$$\bar{f}^* = \mathbf{K}_{ff^*} (\mathbf{K}_{ff} + \sigma_n^2 \mathbf{I})^{-1} \boldsymbol{\eta}, \quad (5)$$

$$\sigma_*^2 = \mathbf{K}_{**} - \mathbf{K}_{ff^*} (\mathbf{K}_{ff} + \sigma_n^2 \mathbf{I})^{-1} \mathbf{K}_{ff^*}^T, \quad (6)$$

where  $\bar{f}^*$  gives the probabilistic approximate predicted value of the transmission efficiency, and  $\sigma_*^2$  gives the uncertainty of the prediction.

#### 1) Kernel function

Commonly used kernel functions are square kernels, that is, SE covariance, Matérn 3/2 kernel, and so on. As square kernels have a low solution complexity and low computational cost, this study applies the square kernel function to the regression analysis, as shown in (7):

$$k_{SE}(\mathbf{x}, \mathbf{x}') = \sigma_f^2 \exp\left(-\frac{1}{2\nu^2} \|\mathbf{x} - \mathbf{x}'\|^2\right). \quad (7)$$

#### 2) Hyperparameters

In GPR, the various parameters and noise  $\sigma_n^2$  in the kernel function are variable and collectively referred to as hyperparameters. The hyperparameters of the covariance function, mean function, and nugget factor are learned by finding the maximum value of the log marginal likelihood function (8) of the training samples  $(\mathbf{x}_{n \times 0}, \boldsymbol{\eta}_{n \times 1})$ , leading to the optimal hyperparameters:

$$\begin{aligned} & \log p(\boldsymbol{\eta} | \mathbf{x}) \\ &= -\frac{1}{2} \boldsymbol{\eta}^T (\mathbf{K}_{ff} + \sigma_n^2 \mathbf{I})^{-1} \boldsymbol{\eta} \\ & - \frac{1}{2} \log |\mathbf{K}_{ff} + \sigma_n^2 \mathbf{I}| - \frac{n}{2} \log 2\pi. \end{aligned} \quad (8)$$

Unconstrained nonlinear optimization algorithms can solve the GPR maximum likelihood estimation problem. Common methods are the conjugate gradient method and quasi-Newton method, but the solution complexity enhances as dimensionality increases. The Fmincon algorithm uses the interior point method, which is highly accurate and converges well but requires a suitable assigned initial value when optimizing. Classical stochastic optimization methods, such as genetic algorithms and particle swarm algorithms, have the advantage of not relying on initial values and using global search for optimality, which are less likely to fall into local optimality but prone to premature convergence and low accuracy [24]. However, the RSA has superior convergence and can improve accuracy [25]. Therefore, in

this study, the RSA is used for the GPR hyperparameter solution and compared with other stochastic optimization algorithms to verify the optimization-seeking capability.

#### A. Sampling strategy for aGPR training

The aGPR method allows the standard deviation  $\sigma_*$  at the transmission efficiency prediction point  $x$  to be the entropy  $IE(x)$ , according to the information entropy adaptive sampling strategy [26], as shown in (9). First, this strategy collects the specified samples from the candidate pool  $X_{cand}$  to the training pool and adds a new input parameter point  $x^{k+1}$  at the maximum value of the transmission efficiency prediction entropy, that is, the maximum standard deviation, as shown in (10), where  $k$  is the number of training samples. Second, the termination condition for the adaptive sampling is determined based on the transmission efficiency prediction accuracy, as shown in (11), which terminates the sampling when the maximum entropy decreases to  $\delta$ . Each iteration fits and constructs a new GP such that the mean of the transmission efficiency prediction points can effectively approximate the true value of the transmission efficiency, maximize the accuracy of the surrogate model, and reduce the required number of training samples. The pseudo-code of aGPR is:

$$IE(x) = \sigma_*, \quad (9)$$

$$x^{k+1} = \underset{x \in X_{cand}}{\operatorname{argmax}} [IE(x)], \quad (10)$$

$$\max [IE(x)] \leq \delta. \quad (11)$$

---

#### Algorithm 1 aGPR training pseudo-code

---

**Input:** Training samples  $\{x_1, \eta_1\}, \{x_2, \eta_2\}, \dots, \{x_n, \eta_n\}$ , testing samples  $\{x_*, \eta_*\}$ , and the maximum entropy  $\delta$

**Output:** The mean and variance of prediction  $\mathbf{f}^*$  and  $\sigma_*^2$

- 1 Initialize the kernel function and the hyperparameters based on (7),(8)
  - 2 **while** sampling isn't finished
  - 3     Calculate the covariance matrices  $\mathbf{K}_{ff}, \mathbf{K}_{**}, \mathbf{K}_{ff^*}$ , the best hyperparameters, the entropy  $IE(x)$  based on (9) and a new input point  $x^{k+1}$  based on (10)
  - 4     **if**  $IE(x) \leq \delta$  **then**
  - 5         Determine the minimum number of adaptive sampling
  - 6     **end**
  - 7     Calculate  $\mathbf{f}^*, \sigma_*^2$  based on (5),(6)
  - 8 **End**
-

In the UQ, most of the initial samples are in the region with a high probability of input parameter distribution, and the entropy of this part of the region is small. In the region with a low probability of input parameter distribution, owing to the lack of sample points, the prediction accuracy is low. Thus, aGPR places most of the adaptive points in the area with a low input parameter probability and continuously reduces the adaptive maximum entropy.

### B. UQ framework based on aGPR

Based on the above theory, this study performs EVWPT system transmission efficiency UQ based on the aGPR surrogate model, which is divided into three main stages.

Stage 1: Preparation of training data

Latin hypercube sampling is used to prepare the training data ( $\mathbf{x}_{n \times \alpha_0} \boldsymbol{\eta}_{n \times 1}$ ). In combination with the actual situation, it is assumed that the spatial misalignment uncertainty input parameters obey a uniform distribution, and the coil structure and component uncertainty input parameters obey a normal distribution, given the mean, variance, and fluctuation range of each parameter.

Stage 2: Construction of aGPR surrogate model

A covariance function is selected for aGPR training, and RSA is used to search for the optimal set of hyperparameters. Let the negative log-likelihood function be the unconstrained minimization objective function and the hyperparameters be the optimization variables to prevent the local optimum. The maximum entropy of the transmission efficiency prediction model is continuously updated, and input parameters from the candidate pool are added to the training pool, iterating until a satisfactory maximum entropy is reached. Model evaluation is performed in comparison with the MC method.

Stage 3: WPT transmission efficiency UQ

Two characteristic statistics of the transmission efficiency model, that is, the mean and variance, and the transmission efficiency are calculated. Based on the results, the impact of the input uncertainty on the output can be understood, and the EV-WPT transmission efficiency uncertainty can be quantified.

## IV. OPTIMIZATION OF EV-WPT TRANSMISSION EFFICIENCY BASED ON RSA

The RSA is a new intelligent optimization algorithm proposed by Laith Abualigah in 2021. The algorithm mainly simulates the hunting behavior of crocodiles to achieve an optimal solution, which has the characteristics of fast convergence and strong search capability [25].

In this study, the RSA is employed to solve two key problems: first, the optimization problem of the GPR machine learning hyperparameters, and second, the EVWPT system structure optimization problem, in

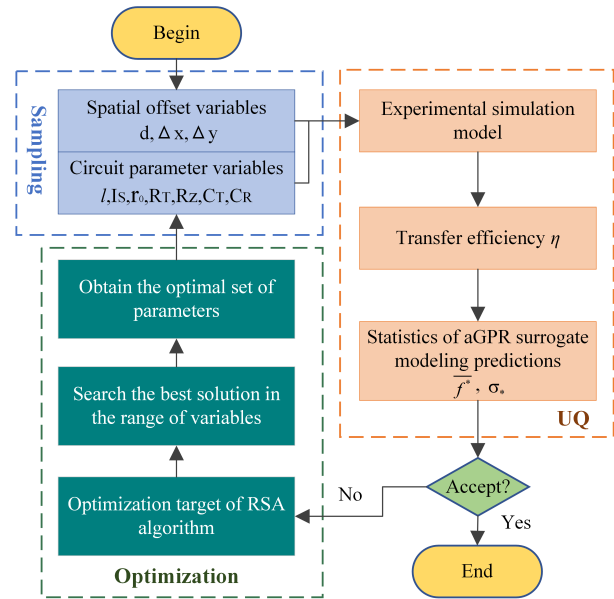


Fig. 4. The overall optimization process for transmission efficiency.

which the WPT system transmission efficiency is taken as the RSA optimization target, and the system structure-related inputs are taken as the optimization parameters to achieve the global optimization of the WPT system transmission efficiency. The overall optimization process is shown in Fig. 4. Firstly, adaptive sampling method is used to extract samples of spatial offset variables and circuit parameters. The aGPR surrogates are then modeled for UQ. The aGPR hyperparameters or model compensation circuit parameters are optimized in the case of unacceptable UQ accuracy and transmission efficiency  $\eta$ . Re-perform the sampling and UQ until the results are acceptable and then end the optimization.

The RSA search process consists mainly of three phases, namely, the initialization phase, encircling phase (exploration), and hunting phase (exploitation).

Initialization phase: The optimization process starts with a set of randomly generated candidate solutions  $X$ , as shown in (12):

$$X = rand \times (UB - LB) + LB, \quad (12)$$

where  $rand$  denotes to a random number between 0 and 1, and  $UB$  and  $LB$  denote the upper and lower bounds of the given problem, respectively.

Encircling phase (global search): The RSA exploration mechanism is based on two main search strategies, that is, the high walking movement strategy and belly walking movement strategy. The high walking strategy depends on  $t \leq T/4$ , the belly walking strategy depends on  $t \leq T/2$ , and  $t > T/4$ . The position update equation for the encircling phase is shown in (13):

$$\begin{aligned}
& x_{(i,j)}(t+1) \\
& = \begin{cases} \text{Best}_j(t) - \gamma_{(i,j)}(t) \times \beta - R_{(i,j)}(t) \times \text{rand}, & t \leq T/4 \\ \text{Best}_j(t) \times x_{(i,j)} \times ES(t) \times \text{rand}, & t \leq T/2 \text{ and } t > T/4 \end{cases}, \quad (13)
\end{aligned}$$

where  $\text{Best}_j(t)$  is the  $i_{th}$  position in the best obtained solution,  $t$  is the number of the current iteration, and  $T$  is the maximum number of iterations. In addition,  $\gamma_{(i,j)}$  denotes the hunting operator for the  $i_{th}$  position in the  $i_{th}$  solution, which is calculated using (14);  $\beta$  is fixed to equal 0.1; the reduce function  $R_{(i,j)}$  is the value used to reduce the search area, which is calculated using (15);  $r_1$  is a random number between  $[1 N]$ ;  $x_{(r_1,j)}$  denotes a random position of the  $i_{th}$  solution;  $N$  is the number of candidate solutions; and  $ES(t)$  is the evolutionary sense, which is calculated using (16):

$$\gamma_{(i,j)} = \text{Best}_j(t) \times P_{(i,j)}, \quad (14)$$

$$R_{(i,j)} = \frac{\text{Best}_j(t) - x_{(r_1,j)}}{\text{Best}_j(t) + \varepsilon}, \quad (15)$$

$$ES(t) = 2 \times r_3 \times \left(1 - \frac{1}{T}\right), \quad (16)$$

where  $\varepsilon$  is a small value,  $r_2$  is a random number between  $[1 N]$ ,  $r_3$  denotes a random integer between  $[-1 1]$ , and  $P_{(i,j)}$  is the percentage difference between the  $j_{th}$  position of the best obtained solution and  $i_{th}$  position of the current solution.

Hunting phase (local search): The RSA exploitation mechanism makes use of the search space and is based on two main search strategies (hunting coordination and cooperation) to avoid getting trapped in the local optima, as shown in (17). The hunting coordination operation depends on  $t \leq 3T/4$  and  $t > T/2$ , and the hunting cooperation operation depends on  $t \leq T$  and  $t > 3T/4$ :

$$\begin{aligned}
& x_{(i,j)}(t+1) \\
& = \begin{cases} \text{Best}_j(t) \times P_{(i,j)}(t) \times \text{rand}, & t \leq \frac{3T}{4} \text{ and } t > \frac{T}{2}, \\ \text{Best}_j(t) - \gamma_{(i,j)}(t) \times \varepsilon - R_{(i,j)}(t) \times \text{rand}, & \\ t \leq T \text{ and } t > \frac{3T}{4}. \end{cases} \quad (17)
\end{aligned}$$

The algorithm produces a random value in each iteration, and this part of searching is beneficial in the case of local optimum stagnation, especially in the final iteration.

## V. EXPERIMENTAL SIMULATION ANALYSIS

### A. UQ of transmission efficiency

Based on the transmission efficiency model in Section II, it was determined that the EV-WPT transmission efficiency was highly uncertain owing to the influence of the coupling mechanism misalignment, uncertainty of the coil structure, and circuit component parameters. Based on the actual situation, it was assumed that the spatial location parameters obeyed a uniform

Table 1: Parameter distribution of random variables

Variables	Random Distribution	Unit
$l$	$N(1, 0.05)$	/
$I_S$	$N(50, 2.5)$	A
$\Delta x$	$U(-0.1, 0.1)$	m
$\Delta y$	$U(-0.1, 0.1)$	m
$d$	$U(0.1, 0.15)$	m
$r_0$	$N(8e-4, 4e-5)$	m
$R_T$	$N(0.1, 0.005)$	$\Omega$
$R_Z$	$N(5, 0.25)$	$\Omega$
$C_T$	$N(120, 6)$	nF
$C_R$	$N(130, 7.5)$	nF

distribution, and the component parameters obeyed a normal distribution. After determining reasonable component parameters, the intervals of the most probable distribution of parameters and possible boundaries of the optimized parameters are determined in conjunction with the real situation. The normal distribution sets the variance to  $0.05 \times \text{mean}$ . The distribution intervals of 10 variables with an impact on transmission efficiency were shown in Table 1.

According to the random distribution parameters in Table 1, 200 training samples were collected with the Latin hypercube sampling method as the initial training pool to establish the aGPR model, and 300 adaptive iterations were performed until the adaptive maximum entropy has leveled off. Another 800 training samples were collected to establish the GPR surrogate model according to the prediction accuracy. At the same time, based on experience and the UQ stability, 10,000 MC simulation experiments were performed to verify the accuracy of the aGPR method. The simulation model took about 1 minute to sample each sample, and the calculation time was given for computers with 6core/12-thread processors (Intel Core i5-10400, 2.90 GHz) and 16 GB of RAM, running Windows.

A square kernel was used as the kernel function to optimize the hyperparameters  $\theta = [v_0 \sigma_f \sigma_k]$  for the establishment of the aGPR model. To verify the tracking performance of the RSA, it was compared with the simulated annealing algorithm, arithmetic optimization algorithm, and other common algorithms [25]. With (8) as the tracking objective, the population size of each algorithm was set to 20, and the maximum number of iterations was set to 100. The convergence behavior and computation time of each algorithm are shown in Fig. 5. The same global optimal solution was obtained for all the methods, except for the GA, which was trapped in a local optimum, and the RSA had a faster search speed than the other methods, took less time to compute, and demonstrated the strongest overall search capability.

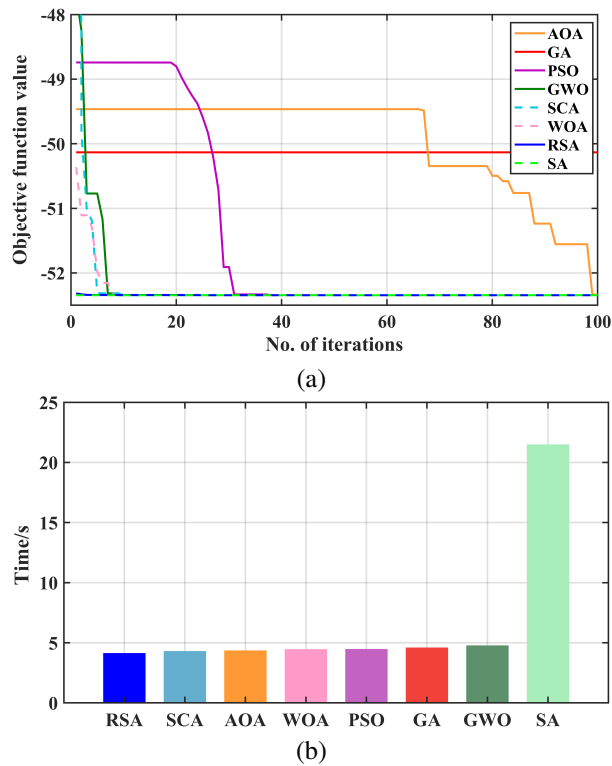


Fig. 5. (a) Convergence results of maximum likelihood estimation and (b) computation time of each algorithm.

To verify whether the aGPR model can overcome the “curse of dimensionality”, UQ was performed on the transmission efficiency of the first five and all 10 dimensions in Table 1, and the training process and prediction results of the five-dimensional variables are shown in Fig. 6. As shown in Fig. 6 (a), the adaptive maximum entropy value decreased continuously during the aGPR training process, and a highly desirable maximum entropy was observed after about 250 calculations. The aGPR prediction results were compared with the true values, as shown in Fig. 6 (b).

The probability of the actual values falling within the prediction interval was 98.75%. Similarly, the GPR prediction results, compared with the true values, are shown in Fig. 6 (c), with a probability of 96.78%, demonstrating that the actual values fell within the prediction interval. To examine the performance of the obtained surrogate model, the aGPR and GPR prediction results were compared, as shown in Fig. 6 (d) and Table 2, demonstrating that the aGPR model had a higher prediction accuracy in the areas with a low probability of occurrence of the samples and stronger predictive capability than the GPR model.

According to the above experiments and EV-WPT model proposed in Section II, this study quantified the uncertainty of the EV-WPT system transmission effi-

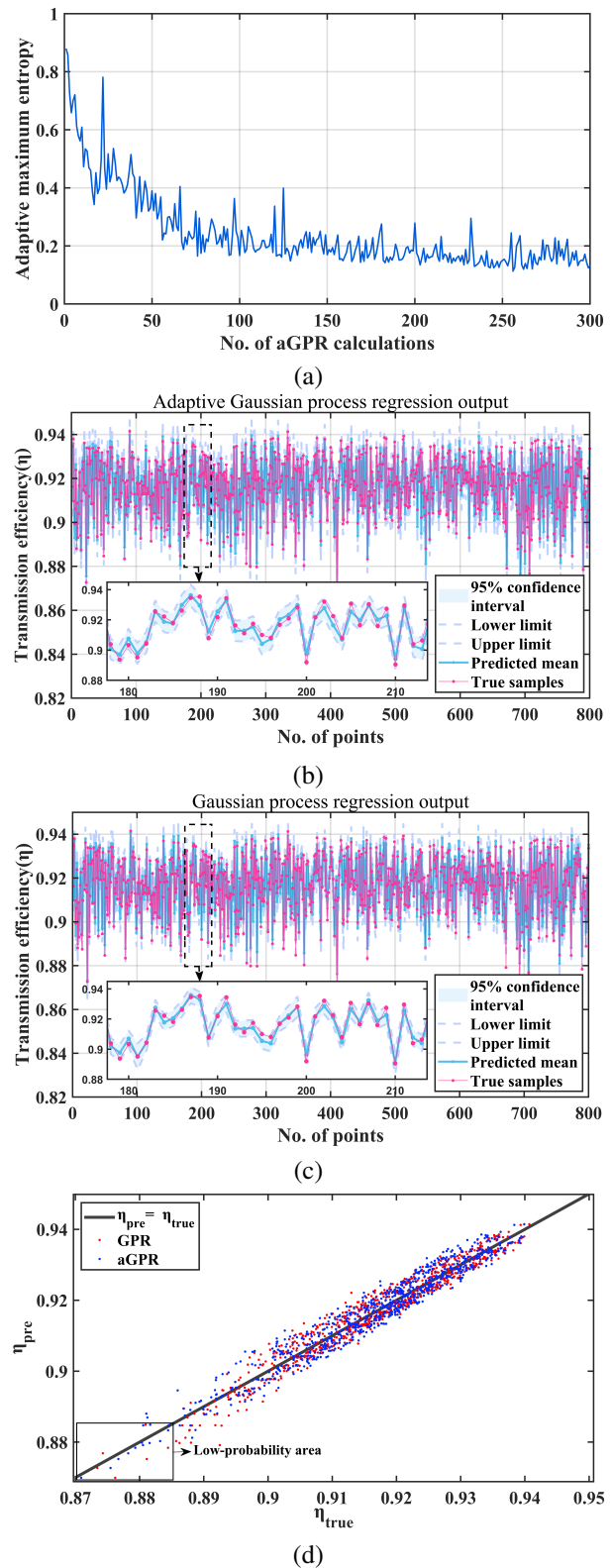


Fig. 6. GPR and aGPR training process and results: (a) Adaptive maximum entropy value iteration, (b) AGPR training and prediction, (c) GPR training and prediction, and (d) Comparison of predicted mean and true values.

Table 2: Statistical parameters related to prediction

	Probability of Actual Values Within the Predicted Intervals	MAPE	RMSE	Coefficient of Determination
GPR	96.78%	0.27%	0.0030	0.97355
aGPR	98.75%	0.27%	0.0029	0.97406

ciency based on the aGPR, GPR, and MC models and obtained the comparison results of the three methods through simulation, as shown in Fig. 7 and Table 3. Based on the above simulation results, it was determined that the UQ accuracy of the proposed aGPR model was basically the same as that of the MC method. Compared with the GPR model, the overall speed of the aGPR model increased by about 9.2% and 14.3%, which substantially reduced the computational cost. The computational cost remained the same when the dimensionality of the input variables increased, indicating that the

aGPR model was not trapped in the “curse of dimensionality”, but the mean value of the transmission efficiency decreased, and the variance increased, showing the existence of many uncertainties in the actual engineering, which can reduce the transmission efficiency and robustness of the WPT system. Therefore, there is an urgent need to optimize EV-WPT systems.

## B. Optimization

In combination with the contents of Section IV, component parameters  $R_T, R_Z, C_T,$  and  $C_R$  in the primary and secondary circuits were optimized, with WPT system efficiency as the optimization objective. With the mean values of the parameters in Table 1 as the basis, optimization was performed within the range of  $[R_T/2, 2 \times R_T], [R_Z/2, 2 \times R_Z], [C_T/2, 2 \times C_T],$  and  $[C_R/2, 2 \times C_R],$  considering the global search and calculation cost.

To verify the superiority of the RSA, it was compared with the Sparrow Search Algorithm (SSA), improved Grey Wolf Optimizer (IGWO), and Enhanced Whale Optimization Algorithm (EWOA) at the same time.

According to the experimental effect, the population size of all four algorithms was 20, and the maximum

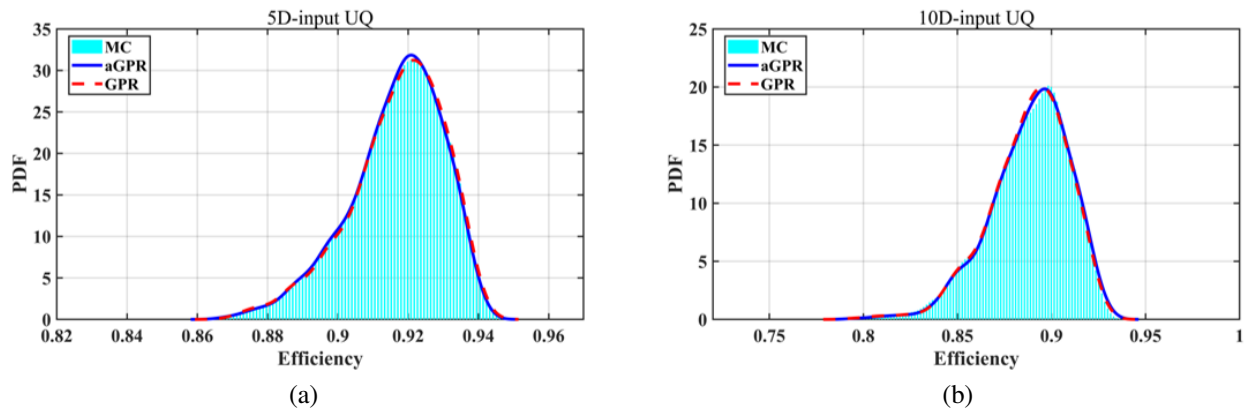


Fig. 7. Contrast of probability density function (PDF) (a) under the first five dimensions and (b) under the whole dimensions of input variables in Table 1.

Table 3: Comparison of MC, GPR, and AGPR models with uncertainty inputs

Dimensions of Variables	Method	Mean	Variance	Correlated Error		Total Time	
				Mean	Variance	Sampling	Calculation
5	MC	0.9044	0.02712	Mean	Variance	6 d22 h	
	GPR	0.9053	0.02662	0.0995%	-1.844%	13 h27 min	53 s
		aGPR	0.9045	0.02678	0.011%	-1.254%	12 h19 min
10	MC	0.8628	0.04578	Mean	Variance	7 d8 h	
	GPR	0.862	0.04822	-0.093%	5.33%	13 h49 min	57 s
		aGPR	0.8629	0.04829	0.012%	5.46%	12 h05 min



number of iterations was 10. The efficiency optimization iterative process and optimization results of each method are shown in Table 4 and Fig. 8. The SSA and EWOA easily fell into local optimization, resulting in low search accuracy. Although the IGWO demonstrated high search accuracy, its calculation speed was slow such that the optimal transmission efficiency of 94.23% was approached in the 8th iteration. Compared with the other algorithms, the RSA had a faster calculation speed and higher search accuracy, which quickly approached the optimal transmission efficiency in the third iteration, and effectively solved the problem of WPT efficiency optimization.

Taking the optimal solution obtained by the RSA as the mean of the input parameters, the probability density function of the transmission efficiency, corresponding to the 10-dimensional uncertainty inputs in Table 1, was calculated by the aGPR model. The mean value of the optimized aGPR prediction was 0.9343, and the variance was 0.02218. The mean value of the transmission efficiency improved by 8.27%, and the variance decreased by 54.07%, which significantly improved the transmission efficiency and robustness of the EV-WPT system, thereby providing a theoretical basis for the practical engineering design and optimization of EVWPT systems. The probability density functions of the efficiency, quantified by the aGPR and

Table 4: Parameter comparison before and after optimization

	$R_T(\Omega)$	$R_Z(\Omega)$	$C_T(\text{nE})$	$C_R(\text{nF})$	$\eta \times 10^0$ (%)
<b>Original</b>	0.1	5	120	130	90.52
<b>RSA</b>	0.1582	9.9962	224.4007	191.5533	94.23
<b>IGWO</b>	0.1525	9.9986	235.4230	194.9361	94.23
<b>EWOA</b>	0.1542	8.2954	119.1866	140.7130	93.15
<b>SSA</b>	0.2	10	240	65	84.50

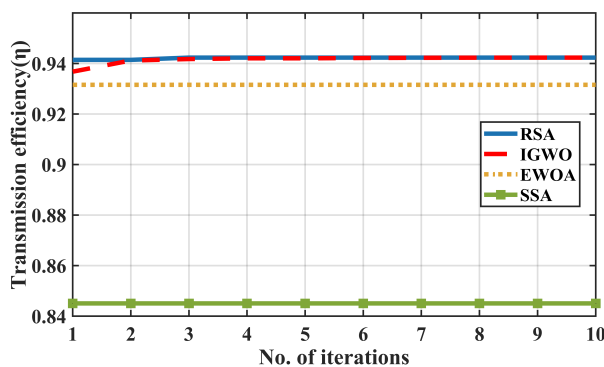


Fig. 8. Comparison of different algorithms for efficiency optimization results of WPT system.

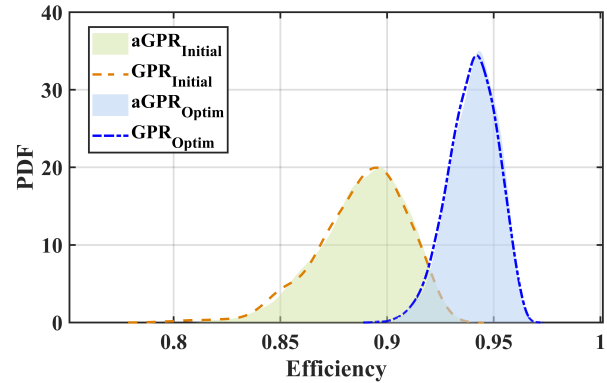


Fig. 9. Comparison of PDFs for efficiency of WPT system before and after optimization.

GPR models before and after optimization, are compared in Fig. 9.

The above simulations and comparative experiments showed that when uncertainties were present in the transmission process, the optimized WPT system proposed in this study demonstrated high transmission efficiency and strong robustness, which can effectively meet practical engineering needs.

## VI. CONCLUSION

Based on the influence of transceiver coil mutual inductance on the transmission efficiency, this study focuses on the uncertainty effect of input variables on the efficiency of an EV-WPT system under actual conditions. In this study, aGPR is proposed as the UQ framework for EV-WPT transmission efficiency. Through a comparison of the quantitative results of the MC, GPR, and aGPR models, it is determined that the aGPR model has approximately the same solution accuracy as the MC method, and its computational speed is about 9.2% better than that of the GPR model, which can significantly reduce the computational cost and verify the absence of the “curse of dimensionality”. The RSA is used to optimize the transmission efficiency, and the results show that the mean value of the optimized transmission efficiency increases by 8.27%, whereas the variance decreases by 54.07%. In summary, the results reveal that the scheme proposed in this study can provide a low-cost and reliable solution for the transmission efficiency UQ and optimization of EV-WPT systems.

## ACKNOWLEDGMENT

This work was supported in part by the Jilin Scientific and Technological Development Program under Grant 20230201122GX, Grant 20220101196JC, and Key Laboratory for Comprehensive Energy Saving of Cold Regions Architecture of Ministry of Education, Jilin Jianzhu University under Grant JLJZHDKF202203.

## REFERENCES

- [1] A. Triviño, J. M. González-González, and J. A. Aguado, "Wireless power transfer technologies applied to electric vehicles: A review," *Energies*, vol. 14, no. 6, p. 1547, Mar. 2021.
- [2] A. Ahmad, M. S. Alam, and R. Chabaan, "A comprehensive review of wireless charging technologies for electric vehicles," *IEEE Trans. Transp. Electrific.*, vol. 4, no. 1, pp. 38-63, Mar. 2018.
- [3] S. Y. Choi, B. W. Gu, S. Y. Jeong, and C. T. Rim, "Advances in wireless power transfer systems for roadway-powered electric vehicles," *IEEE J. Emerg. Sel. Topics Power Electron.*, vol. 3, no. 1, pp. 18-36, Mar. 2015.
- [4] D. Patil, M. K. McDonough, J. M. Miller, B. Fahimi, and P. T. Balsara, "Wireless power transfer for vehicular applications: Overview and challenges," *IEEE Trans. Transp. Electrific.*, vol. 4, no. 1, pp. 3-37, Mar. 2018.
- [5] K. Detka and K. Górecki, "Wireless Power Transfer-A Review," *Energies*, vol. 15, no. 19, p. 7236, Jan. 2022.
- [6] M. G. Eftekhari, Z. Ouyang, M. A. E. Andersen, P. B. Andersen, L. A. de S. Ribeiro, and E. Scholtz, "Efficiency study of vertical distance variations in wireless power transfer for e-mobility," *IEEE Trans. Magn.*, vol. 52, no. 7, pp. 1-4, July 2016.
- [7] H. Kim, C. Song, H. Kim, D. H. Jung, I.-M. Kim, Y.-I. Kim, J. Kim, S. Ahn, and J. Kim, "Coil design and measurements of automotive magnetic resonant wireless charging system for high efficiency and low magnetic field leakage," *IEEE Trans. Microw. Theory Techn.*, vol. 64, no. 2, pp. 383-400, Feb. 2016.
- [8] R. Narayanamoorthi, "Modeling of capacitive resonant wireless power and data transfer to deep biomedical implants," *IEEE Trans. Compon. Packag. Manuf. Technol.*, vol. 9, no. 7, pp. 12531762Tule20710.
- [9] G. Fishman, *Monte Carlo: Concepts Algorithms and Applications*, Berlin: Springer, 2013.
- [10] M. Rossi, G.-J. Stockman, H. Rogier, and D. Yande Ginste, "Stochastic analysis of the efficiency of a wireless power transfer system subject to antenna variability and position uncertainties," *Sensors*, vol. 16, no. 7, pp. 1100, July 2016.
- [11] Q. Yu, W. Liu, K. Yang, X. Ma, and T. Wang, "Uncertainty quantification of the crosstalk in multiconductor transmission lines via degree adaptive stochastic response surface method," *Applied Computational Electromagnetics Society (ACES) Journal*, vol. 36, no. 2, pp. 174-183, Mar. 2021.
- [12] R. Trincherro, M. Larbi, H. M. Torun, F. G. Canavero, and M. Swaminathan, "Machine learning and uncertainty quantification for surrogate models of integrated devices with a large number of parameters," *IEEE Access*, vol. 7, pp. 4056-4066, 2019.
- [13] M. Larbi, R. Trincherro, F. G. Canavero, P. Besnier, and M. Swaminathan, "Analysis of parameter variability in an integrated wireless power transfer system via partial least-squares regression," *IEEE Trans. Compon. Packag. Manuf. Technol.*, vol. 10, no. 11, pp. 1795-1802, Nov. 2020.
- [14] Y. Pei, L. Pichon, M. Bensetti, and Y. Le-Bihan, "Uncertainty quantification in the design of wireless power transfer systems," *Open Phys.*, vol. 18, no. 1, pp. 391-396, July 2020.
- [15] T. Wang, Y. Wu, B. Li, Q. Yu, L. Xu, and S. Guan, "Design of electric vehicle's wireless power transfer system based on deep learning combined with multi-objective optimization," *IEEE Trans. Compon. Packag. Manuf. Technol.*, vol. 12, no. 12, pp. 1983-1994, Nov. 2022.
- [16] P. Manfredi and R. Trincherro, "A probabilistic machine learning approach for the uncertainty quantification of electronic circuits based on Gaussian process regression," *IEEE Trans. Comput.-Aided Design Integr. Circuits Syst.*, vol. 41, no. 8, pp. 2638-2651, Aug. 2022.
- [17] L. Chen, S. Liu, Y. C. Zhou, and T. J. Cui, "An optimizable circuit structure for high-efficiency wireless power transfer," *IEEE Trans. Ind. Electron.*, vol. 60, no. 1, pp. 339-349, July 2013.
- [18] L. Yang, M. Zong, and C. Li, "Voltage-gain design and efficiency optimization of series/series-parallel inductive power transfer system considering misalignment issue," *Energies*, vol. 14, no. 11, p. 2999, Jan. 2021.
- [19] Z. Zhou, Z. Liu, and H. Su, "Multi-objective optimization of the wireless power transfer system for electric vehicles," in *Proc. IEEE Wireless Power Transf. Conf. (WPTC)*, pp. 215-218, Nov. 2000.
- [20] S. Jeong, J. Jung, K. A. Kim, and J. Kim, "Analytical investigation of optimal wireless power transfer topology for electric vehicles," in *Proc. IEEE PELS Workshop Emerg. Technol. Wireless Power (WoW)*, pp. 1-5, June 2015.
- [21] Y. Guo, L. Wang, and C. Liao, "A general equivalent model for multi-coil wireless power transfer system analysis and its application on compensation network design," *Applied Computational Electromagnetics Society (ACES) Journal*, vol. 33, no. 06, pp. 648-656, July 2021.

- [22] C. E. Rasmussen and C. K. I. Williams, *Gaussian Processes for Machine Learning*, Cambridge, MA: MIT Press, 2006.
- [23] T. Zhang, Y. Tian, X. Chen, and J. Gao, "Antenna resonant frequency modeling based on AdaBoost gaussian process ensemble," *Applied Computational Electromagnetics Society (ACES) Journal*, vol. 35, no. 12, pp. 1485-1492, Dec. 2020.
- [24] C. Rong, X. He, Y. Wu, Y. Qi, R. Wang, Y. Sun, and M. Liu, "Optimization design of resonance coils with high misalignment tolerance for drone wireless charging based on genetic algorithm," *IEEE Trans. Ind. Appl.*, vol. 58, no. 1, pp. 12421253, Jan. 2022.
- [25] L. Abualigaha, M. A. Elaziz, P. Sumari, Z. WooGeem, and A. H. Gandomi, "Reptile Search Algorithm (RSA): A nature-inspired metaheuristic optimizer," *Expert Syst. Appl.*, vol. 1, Apr. 2022.
- [26] J. Zhou and J. Li, "IE-AK: A novel adaptive sampling strategy based on information entropy for Kriging in metamodel-based reliability analysis," *Reliab. Eng. Syst. Saf.*, vol. 229, p. 108824, Jan. 2023.



**Xinlei Shang** received the B.S. degree, the M.S. degree and the Ph.D. degree in Test and Measurement Technology and Instrumentation from Jilin University, Changchun, Jilin, China, in 2004, 2007 and 2010, respectively.

He is currently a professor with the College of Instrumentation and Electrical Engineering, Jilin University. His research interest includes nuclear magnetic resonance and transient electromagnetism.



**Linlin Xu** received the B.S. degree in electrical engineering and automation from the College of Instrumentation and Electrical Engineering, Jilin University, Changchun, Jilin, China, in 2020, where she is currently pursuing the M.S. degree in electrical engineering.

ing.

Her research interests include electromagnetic safety and electromagnetic compatibility of wireless charging systems in electric vehicles.



**Quanyi Yu** received the B.S. degree from the College of Communication Engineering, Jilin University, Changchun, Jilin, China, in 2016, the M.S. degree from College of Instrumentation and Electrical Engineering, Jilin University, Jilin, China, in 2020, where he is currently pursuing the Ph.D. degree in measurement technology and instruments.

His research interests include the uncertainty quantification and electromagnetic compatibility of wireless power transfer of EVs.



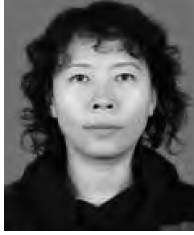
**Bo Li** received a B.S. degree in electrical engineering and automation from College of Instrumentation and Electrical Engineering, Jilin University, Changchun, Jilin, China, in 2020. He is currently studying for a M.S. degree in electrical Engineering from the College of Instrumentation and Electrical Engineering, Jilin University.

His research interests include uncertainty analysis, wireless power transfer, magnetic resonance, and human protection.



**Gang Lv** received the master degree of electronic circuit and system in college of electronic science & engineering, Jilin University, Changchun, Jilin, China, in 2008. He came on board into National Automotive Quality supervision & Inspection Center (Changchun) after graduated. He is currently the head of the EMC department. He is mainly in charge of the EMC performance in vehicle type approval under the direction of Ministry of Industry and Information Technology (MIIT) and Certification and Accreditation Administration of the P.R.C.

He always focuses on test methods improving and National Standards edit and amendment in EMC domain. He has joined teams to be responsible for EMC part of "Test and Evaluation of autonomous electric vehicle" subject which is released by Ministry of Science and Technology (MOST) and "Research on real-time concurrent Simulation test technology of Multi-source Sensor information of Intelligent Networked Vehicle" which is released by Science and Technology Department of Jilin Province.



**Yaodan Chi** received the B.S. degree in electronic information engineering from the Jilin University of Technology, Changchun, Jilin, China, in 1998, and the master's degree in testing and measuring technology and instruments and the Ph.D. degree in science and technology of instrument from Jilin University, Changchun, Jilin, China, in 2004 and 2018, respectively. She is currently the Vice Director of the Jilin Provincial Key Laboratory of Architectural Electricity and Comprehensive Energy Saving.

Her research interests include the uncertainty analysis approaches in electromagnetic compatibility simulation and building equipment intelligent integration technology.



**Tianhao Wang** received the B.S. degree in electrical engineering and the Ph.D. degree in vehicle engineering from Jilin University, Changchun, Jilin, China, in 2010 and 2016, respectively.

From 2016 to 2019, he was a Postdoctoral Researcher with the Department of Science and Technology of Instrument, Changchun, Jilin University. He is currently an associate professor with the College of Instrumentation and Electrical Engineering, Jilin University. His research interest includes the uncertainty quantification of wireless power transfer of EVs and human electromagnetic exposure safety.